J Solid State Electrochem (1998) 2: 242–246

ORIGINAL PAPER

Ariyanan Mani · Subramanian Tamil Selvan
Kanala Lakshminarasimha Phani

Solid state structural aspects of electrochemically prepared poly (*p*-phenylene) thin films – crystalline order and spherulite morphology

Received: 29 July 1997 / Accepted: 27 October 1997

Abstract The electrochemical polymerization of benzene via the microemulsion approach yields highly crystalline and anisotropic "spherulitic" polyparaphenylene (PPP) thin films. The crystalline order and the origin of spherulite morphology are discussed.

Key words Polyparaphenylene (PPP) · Crystalline order · Spherulites

Introduction

Micellar and microemulsion media are being widely employed for the synthesis of polymer microstructures [1]. Microemulsions are microheterogeneous media enabling higher solubility and the possibility of the surfactant monolayers acting as "templates" for synthesizing various organic and inorganic microstructures. As proposed by Rusling [2], a few monolayers of the surfactant are formed on the electrode surface with well-defined microstructures, and these could serve as "templates" for the electrochemical reactivity. We have earlier reported the possibility of electrosynthesizing polyparaphenylene from an oil-in-water type microemulsion medium stabilized by sodium dodecylsulfate surfactant. The crystalline order and the evolution of morphology during electropolymerization were reported by us in a preliminary note [3]. There is a widespread realization that polymerization in such organized media provides an exciting possibility of controlling the polymer microstructures. As materials science seeks control of structure and properties (short- or long-range order), polymerization in anisotropic phases such as micelles is sure to take on increasing importance [4].

A. Mani · S.T. Selvan · K.L. Phani (✉)
Central Electrochemical Research Institute,
Karaikudi – 630 006, India
Tel.: +91-04565-22322; Fax: +91-04565-22088;
e-mail: cecrik@cscecri.ren.nic.in

During recent years, conjugated polymers have become attractive materials for electroluminescent devices and photoconductors [5–9]. Among various candidate polymers, polyparaphenylene (PPP) and its substituted analogues are recognized for their good stability and conductivity, rendering them suitable for the above-mentioned device applications. The significance of controlling the polymer morphology has also been highlighted in several publications [10–13].

In conjugated polymers, the electron- as well as ion-transport properties strongly depend on their solid-state structural aspects, particularly crystalline order and morphology. For example, electrical conductivity is largely controlled by interchain charge transport, which mainly depends on the alignment of the macromolecular chains in the film matrix, and the rate of doping and dedoping depend on polymer morphology [14]. Although many reports are available in the literature on the synthesis and properties of PPP [15–17], the aspects concerning its crystalline characteristics and their relation to its morphology have not been dealt with. In this paper, we report crystallographic details and morphological features of PPP thin films deposited by electrochemical oxidation of benzene by potentiodynamic cycling.

Experimental

PPP thin films were synthesized by a method similar to our earlier procedure [9–10]. The benzene monomer was solubilized in conc. H_2SO_4 (18 M) using Triton X-100 (14.8 mM), thus yielding an oil-in-water type microemulsion, and the optimum benzene:H_2SO_4 ratio of 2:5, corresponding to 70 ml of microemulsion, was directly used as an electrolysis medium. The PPP films were grown on indium-tin-oxide (ITO) glass (1 cm^2) by cycling between −0.21 and + 0.91, V vs Hg/Hg_2SO_4/1 M H_2SO_4 (MSE) with a scan rate of 100 mV s^{-1} at ambient temperature. The film thickness (t) values are expressed in terms of the anodic charge consumed in the cyclic potentiodynamic growth pattern (mC cm^{-2}), i.e., the first 20 cycles correspond to 2.35 mC cm^{-2}, 12 cycles to 1.38 mC cm^{-2}, and 23–40 cycles to higher thickness values in the range of $5.75 > t > 2.35$ mC cm^{-2}. The PPP films after electrochemical

cycling were washed with water and ethanol before recording X-ray diffraction (XRD) patterns and microstructures.

The XRD patterns were recorded using computer-controlled X-ray powder (wide-angle) diffractometer system JEOL-JDX 8030 at a rating of 40 kV, 20 mA with Ni-filtered CuKα radiation (λ = 0.15418 nm). The θ–2θ scan mode was used to scan the polymer film samples between 3 and 65°–2θ at a step-scan of 0.1°–2θ with a measuring time of 1s per step. The digitized XRD scan was processed using the standard software available with the system, and plotter outputs were taken using a GRAPHTEC plotwriter, model WX4731.

The morphology of PPP thin films was examined using a JEOL JSM-35CF scanning electron microscope (SEM).

Results and discussion

The XRD patterns of PPP films of different thickness values (mC cm^{-2}) are presented in Fig. 1. The three patterns indicate perfect crystalline, intermediate semi-crystalline, and amorphous characteristics, corresponding to the polymer thickness values of 1.38, 2.65 and 5.75 mC cm^{-2} respectively. In the first case (Fig. 1a), the degree of crystallinity has been found to be 99%. This is due to perfect long-range ordering of the polymer chains. As the thickness increases to >2.35 mC cm^{-2}, the orderly stacking of polymer chains is disturbed; the crystalline order decreases to 68% because random arrangement of the polymer chains sets in, as in the case of foldings. At still higher thickness, for example 5.75 mC cm^{-2}, the crystallographic order totally vanishes and only the randomness results.

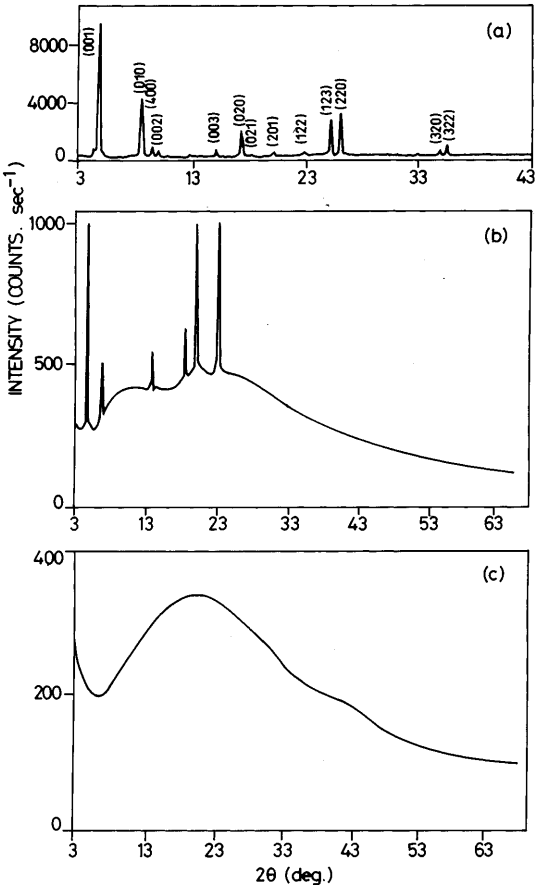

Fig. 1a–c X-ray powder diffraction patterns of PPP thin films of different thicknesses obtained by potentiodynamic cycling in microemulsion (with Triton X-100) medium: **a** 1.38, **b** 2.65 and **c** 5.75 mC cm^{-2}. Degree of crystallinity values are 99, 68 and 0% respectively

The long-range crystalline order of the polymer films has been indexed in the orthorhombic crystal lattice. The literature data and the present XRD data are compared in Table 1. The present XRD data include the low-angle peaks or higher lattice constants which have not hitherto been observed or accounted for. The higher-angle peaks were indexed using the values reported elsewhere [18]. The newly observed low-angle XRD peaks could not previously be explained by us [3]. However, these lines have now been explained in the new orthorhombic unit cell. Both the lattice parameters are presented in Table 2. It is envisaged that the presently reported large unit cell volume (nearly ten times larger) can accommodate more polymer chains of the PPP macromolecules with more orderly packing giving rise to greater crystalline order.

At the intermediate stage (Fig. 1b), the orthorhombic symmetry seems to have been disturbed so as to conform to a low-symmetry lattice, probably monoclinic, as can be seen in the low-angle region of the XRD pattern. The absence of peaks at higher angles indicates that the long-

Table 1 X-ray powder diffraction data for PPP thin films. vs, very strong; s, strong; m, medium; w, weak; vw, very weak

d (obsd.) (nm)	(hkl)		Relative intensity	
	Literature [3, 18]	Present	Obsd.	I/I_0
1.7659	–	(001)	vs	100
1.0273	–	(010)	s	34
0.9111	–	(100)	m	12
0.8838	–	(002)	vw	5
0.5901	–	(003)	w	7
0.5151	(010)	(020)	m	18
0.4792	–	(021)	vw	6
0.4414	(110)	(201)	>w	6
0.3897	(101)	(122)	>w	8
0.3545	–	(123)	>m	27
0.3424	(011)	(220)	m	26
0.2918	–	(033)	vw	5
0.2583	(020)	(321)	w	6
0.2527	(211)	(322)	>w	8

Table 2 Comparison of crystal lattice parameters of PPP

Orthorhombic		Monoclinic
Literature [3, 18]	Present	Literature [18]
a = 0.787 nm	a = 0.9104 nm	a = 0.787 nm
b = 0.519 nm	b = 1.0278 nm	b = 0.517 nm
c = 0.429 nm	c = 1.7661 nm	c = 0.432 nm
		β = 105.7°
V = 0.1752 nm^3	V = 1.6526 nm^3	V = 0.1692 nm^3

range order is disturbed at a thickness value corresponding to 2.65 mC cm^{-2} ($t > 2.35$ mC cm^{-2}). In the third case (Fig. 1c), only the amorphous (non-crystalline) phase is seen. There complete disorder exists at a film thickness of 5.75 mC cm^{-2}.

It is intriguing to ask why crystallinity should decrease in an initially crystalline polymer layer with increase in thickness. The crystallinity in thin films of thickness (t) values $\leqslant 2.35$ mC cm^{-2} is due to the polymer macromolecular order and its packing (on the crystalline substrate such as ITO), as indicated by sharp XRD reflections belonging to the orthorhombic PPP lattice. At $t > 2.35$ mC cm^{-2}, i.e. in the range of $5.75 > t > 2.35$ mC cm^{-2}, the crystalline ordering of the macromolecules is lost, becoming amorphous, which is a bulk characteristic. If cycling is stopped at higher thickness values ($t > 2.35$ mC cm^{-2}) and restarted, the amorphous (bulk) layer continues to grow. But when the electrochemical cycles are stopped before reaching the critical thickness value and restarted, the crystalline film continues to grow as such up to the critical thickness. After the critical thickness, there may exist a small intermediate region of decreasing crystallinity; beyond this region, the films are observed to be completely amorphous, up to $t = 5.75$ mC cm^{-2}, up to which the electrochemical experiments are carried out.

The corresponding SEM micrographs of the PPP films at different stages are shown in Fig. 2. The highly crystalline PPP film (99% crystallinity) exhibits a well-ordered and well-defined "spherulite" morphology as can be seen in the micrograph in Fig. 2c. To our knowledge, this is the first reported observation of the spherulite morphology of the highly ordered PPP thin films obtained by microemulsion-based electrosynthesis, although such observations are commonly reported in melt-grown polymers [19]. The spherulite morphology, seen to be distinctly different from other microstructures, reveals the radial fibrils manifesting the supermolecular order of the PPP macromolecular chains within the polymer thin films. In a spherulite, radial fibrils (like spokes of a bicycle wheel) can be seen emanating in all directions from the centre of the spherulite.

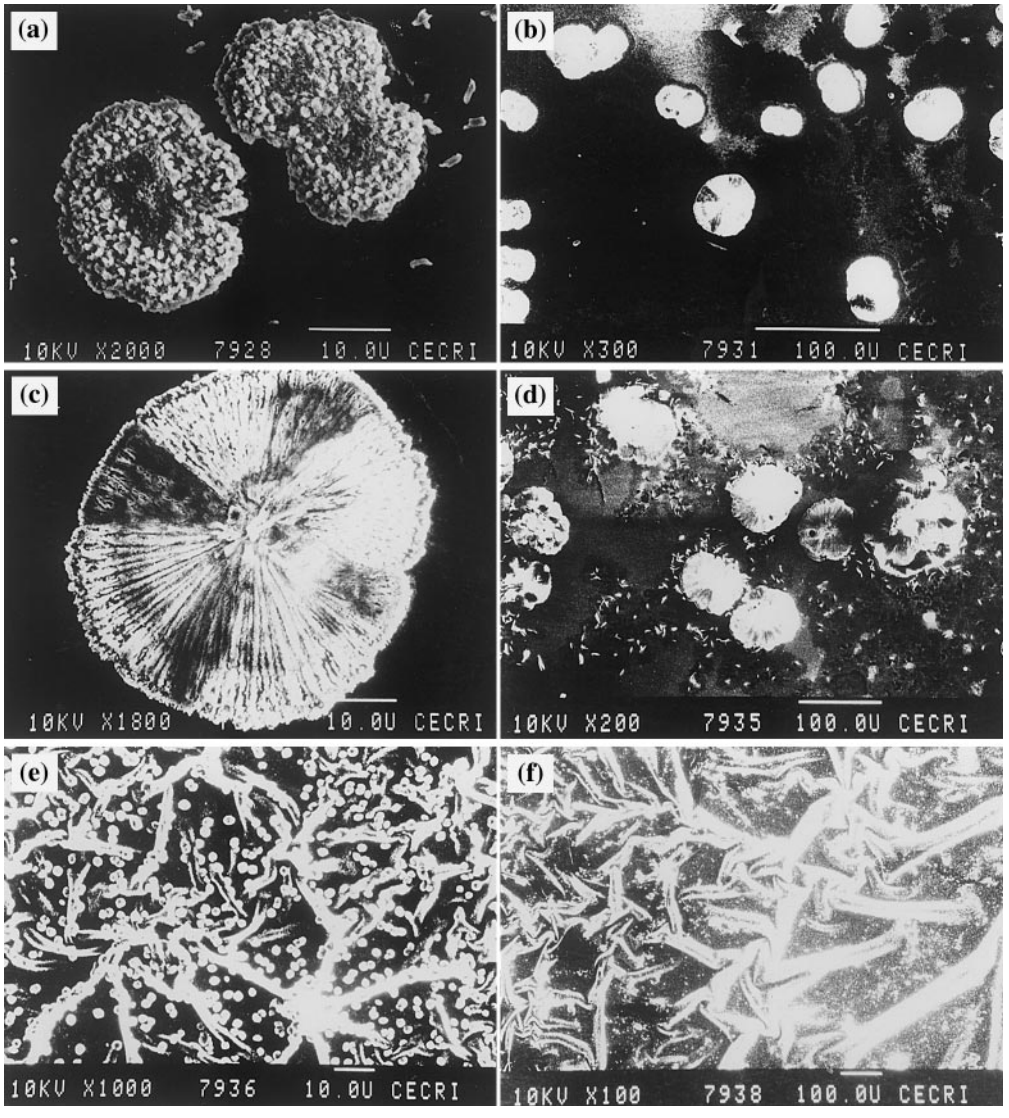

Fig. 2a–f SEM pictures of PPP thin films: **a** spherulites with random crystals at 0.58 mC cm^{-2} oriented spherulite population at 1.38 mC cm^{-2} (lower magnification), **c** same as in **b** at higher magnification elucidating individual spherulite with radial fibrils, **d** "discontinuous" spherulites at 2.65 mC cm^{-2} (corresponding to Fig. 1b), **e** random network and globular features at 3.45 mC cm^{-2} and **f** random network structure at 5.75 mC cm^{-2}

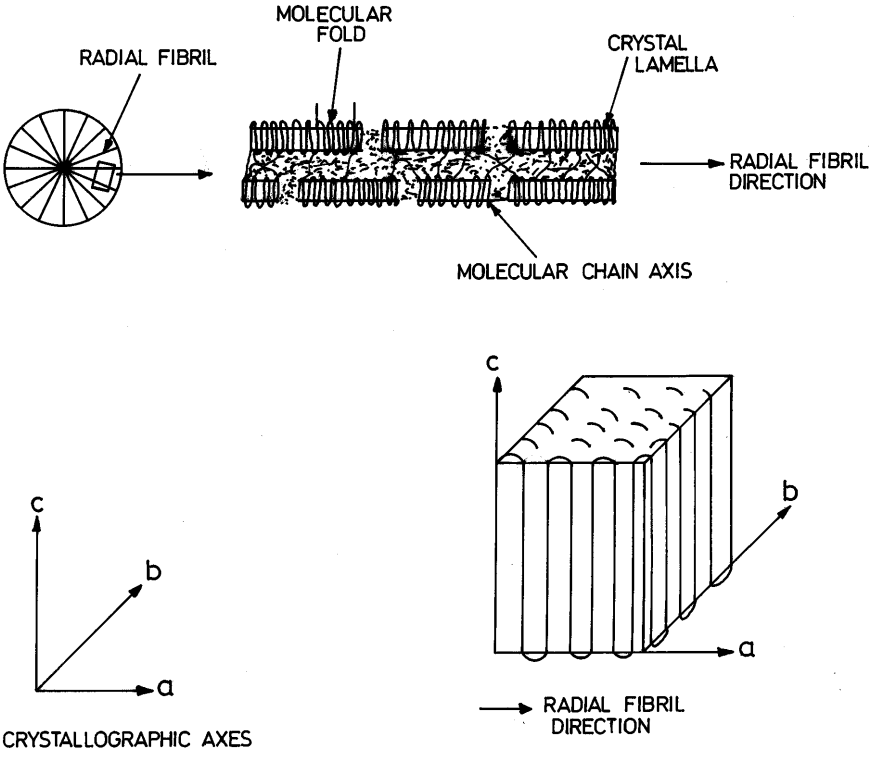

Fig. 3 Schematic of spherulite with radial fibrils and the arrangements of polymer macromolecules within each radial fibril, with respect to common crystallographic reference

They extend outwards until they reach a boundary which may meet an adjacent spherulite or sudden termination of the growth process. The spherulitic nucleation and growth phenomena occur randomly throughout the crystallizing media, mainly by melt processing and possibly also by electrochemical processing. This is the reason for the random location of spherulites in polymers (Fig. 2a, b).

It may be noted that there exist definite crystallographic characteristics of the spherulite morphology. The schematic diagram shown in Fig. 3 illustrates the "zooming up" of the nanoscopic details of the PPP spherulites. The spherulitic *a* axis (fast-growth direction), being parallel to the crystallographic *a* axis, grows radially outward from the nucleating centre of the spherulite, and this results in a specific arrangement of the crystalline region coexisting with the non-crystalline material. The wider the radial fibril along the *b* axis, the higher will be the degree of crystallinity. The *c* direction indicates the thickness of the spherulite.

Each radial fibril is essentially a single crystal [19]. As the spherulite forms, the axis of the crystal is aligned parallel to the radial-fibril axis. Thus all the crystals (i.e., radial fibrils) along each "spoke" in the spherulitic "wheel" have a specific alignment with respect to the other crystals within the spherulite. Now, looking at the PPP radial fibril in more detail, folded-chain crystallites are seen aligned with their *a* axis parallel to the radial-fibril direction (Fig. 3). These crystals seem to be connected (both along and between radial fibrils) through molecules that enter into the crystallization process.

The non-crystalline component (non-uniform, random folding of the PPP molecules) of the polymer is arranged around the growing crystals, and is composed of polymer that cannot enter the crystal lattice. In addition, secondary crystallization occurs between the radial fibrils, both as the spherulites grow and after they reach a maximum limiting size. This leads to random crystal growth in the region between radial fibrils with no long-range order. In the case of "distorted" [3] and "discontinuous" spherulites (Fig. 2d), this kind of short-range order fibrils do exist. This is the situation in the case of intermediate semi-crystalline PPP films, in which the degree of crystalline order is 68%. In the case of completely amorphous PPP thin films (>2.65 mC cm^{-2}), the SEM microstructure is a completely random network structure, as seen clearly in Fig. 2e, f, and is different from the spherulite morphology (Fig. 2b, c), which exhibits supermolecular order.

It is emphasized that supramolecular order (within the molecular chain) of the conjugated polymers contributes to better optical and transport properties. For example, studies in [20] indicate that thiophene oligomers with a photochromic molecular structure can work as insulating/conducting photoswitches. In the insulating (amorphous) "open ring" situations, the thiophene rings are in a twisted conformation and are not in a π-conjugated system. Irradiation closes the ring, causing the four double bonds in the newly closed ring to become conjugated (crystalline) making the polymer conducting. Hence, for improved optical and charge transport properties, higher conjugation length without

defects to allow them to organize in well-ordered structures must be obtained [21].

It is believed that monolayers of the surfactant microstructures that form on the electrode surface can direct the polymerization route and also aid the crystallization process, which will lead to a remarkable improvement in the structural organization of molecules at a mesoscopic level. Alkyl-alkyl recognition phenomena, based on hydrophobic-lipophobic interactions, are strong enough to ensure long-range order. The emission and transport characteristics of the films with such order are bound to improve, as observed by Inganäs et al. [22].

Conclusions

The PPP films, electrosynthesized via the microemulsion route, exhibit excellent long-range crystalline order, orthorhombic unit cell values being $a = 0.9104$, $b = 1.0278$ and $c = 1.7661$ nm. The spherulite morphology with radial fibrils corresponding to a higher degree of crystallinity manifests supermolecular order. With different electrochemical conditions, changes in degree of crystalline order and morphology are also reported. Detailed structural aspects of PPP warrant a separate study. The relationship between the crystal and molecular structural details of the PPP polymers and their optical/transport properties will be an interesting subject of study, and further work is in progress.

Acknowledgements The work reported in this paper is supported by the Department of Science & Technology, New Delhi (SP/S1/H-11/95). The authors thank Mr. P. Kamaraj for his assistance in the SEM work and the referees for useful comments, which have helped in improving the contents of the paper.

References

1. Phani KLN, Pitchumani S, Ravichandran S, Tamil Selvan S, Bharathey S (1993) J Chem Soc Chem Commun 179
2. Rusling JF (1991) Acc Chem Res 24: 75
3. Tamil Selvan S, Mani A, Pitchumani S, Phani KLN (1995) J Electroanal Chem 384: 183
4. Committee on Polymer Science and Engineering, USA (1994) Polymer science and engineering – the shifting research frontiers. National Academy Press, Washington, D.C.
5. Gustafsson G, Gao Y, Treacy GM, Klavetter F, Colaneri N, Heeger AJ (1992) Nature 357: 477
6. Grem G, Leditzky G, Zellrich B, Leising G (1992) Adv Mater 4: 36
7. Graupner W, Leising W, Lanzani G, Nisoli M, De Selvestri S, Scherf U (1995) Phys Lett 246: 95
8. Inganäs O, Berggren M, Anderson MR, Gustaffson G, Hjerberg T, Wennerstrom O, Pyrekla P, Granstrom M (1995) Synth Met 71: 2121
9. Galvai ME (1997) JOM 49: 52
10. Sabatani E, Redondo A, Rishpon J, Rudge A, Robinstein I, Gottesfeld S (1993) J Chem Soc Faraday Trans 89: 287
11. Grandstrom M, Berggren M, Inganäs O (1995) Science 267: 1479
12. Martin CR, Van Dyke LS (1992) In: Murray RW (ed) Techniques of chemistry series, vol 22. Wiley, New York
13. Armes SP (1996) Current Opinion in Colloid & Interface Science 1: 214 and references therein
14. Miyashita K, Kaneko M (1996) J Electroanal Chem 403: 53
15. Kovacic P, Jones MB (1987) Chem Rev 87: 357
16. Yamamoto T, Morita A, Miyazaki Y, Maruyama T, Wakayama H, Zhou ZH, Nakkamura Y, Sasaki S, Kubota K (1992) Macromolecules 25: 1214
17. Goldenberg LM, Lacaze PC (1993) Synth Met 58: 271
18. Baughman RH (1986) In: Skotheim TA (ed) Handbook of conducting polymers, vol 1. Dekker, New York
19. Samuels RJ (1974) Structured polymer properties. Wiley, New York
20. Saika T, Irie M, Shimidzu T (1994) J Chem Soc Chem Commun: 2123
21. Fox KC (1994) New Scientist 369: 33
22. Dyreklev P, Berggren M, Inganäs O, Andersson MR, Wennerström O, Hjertberg T (1995) Adv Mater 7: 43